The International Journal of Advanced Manufacturing Technology (2024) 134:5615–5629
https://doi.org/10.1007/s00170-024-14483-x

ORIGINAL ARTICLE

Mechanical characterization of FDM components made of polyaryletherketone (PAEK) for aerospace applications: a comparison of direct printing and box-cut sample manufacturing strategies

Silvia Ilaria Scipioni[1] · Francesco Pace[1] · Alfonso Paoletti[1] · Francesco Lambiase[1,2]

Received: 27 June 2024 / Accepted: 15 September 2024 / Published online: 23 September 2024

Abstract
This study delves into the manufacturing strategies employed for fabricating tensile samples utilized in the mechanical characterization of material extrusion (MEX) components constructed with polyaryletherketone (PAEK) for aerospace applications. Two distinct methods were investigated for obtaining tensile test samples: direct cutting and extraction from a box. These methods were examined under both as-printed and annealing conditions. Quasistatic tensile tests were conducted along the building direction to evaluate the impact of processing conditions on the adhesion of overlying layers. The results unveiled significant disparities in mechanical behavior and crystallinity between directly printed samples and those derived from the box. The Young's modulus exhibited marginal influence; however, the tensile strength of directly printed samples measured at 30 MPa (prior to annealing), corresponding to 50% of the strength observed in samples cut from the box (60 MPa). Moreover, the elongation at rupture of directly printed samples was found to be less than 2%, while that of cut samples exceeded 8%. Notably, directly printed samples exhibited a significant degree of incipient crystallization (12.18%), contrasting with the lower level of crystallinity observed in samples cut from the box (3.27%). These findings underscore the importance of recognizing the limitations associated with direct sample printing, emphasizing its crucial role in accurately characterizing components destined for the aerospace industry. Furthermore, this understanding is pivotal for optimizing the performance and reliability of MEX-printed PAEK components in aerospace engineering applications.

Keywords Additive manufacturing · FDM · Material extrusion · Mechanical characterization · PEEK · Interlayer adhesion · Aerospace

1 Introduction

In the realm of aerospace engineering, the pursuit of lightweight, durable, and high-performance materials is ongoing. Tecnopolymers have emerged as promising candidates to meet these stringent demands due to their exceptional mechanical properties, thermal stability, and chemical resistance [1–7]. Tecnopolymers, also known as engineering polymers or high-performance polymers, represent a diverse class of synthetic materials engineered to exhibit superior properties compared to traditional polymers [8].

The application of tecnopolymers in aerospace extends across a myriad of components and systems, including structural elements, thermal protection systems, and electrical insulation. From lightweight carbon fiber-reinforced polymers (CFRP) [9–12] for aircraft fuselages to heat-resistant polyetheretherketone (PEEK) composites [13–15] for engine components, tecnopolymers are integral to enhancing efficiency, reliability, and safety in aerospace operations. The limited production volumes required in the aerospace sector frequently result in the adoption of tecnopolymers becoming prohibitively expensive [1, 2]. This challenge is not unique to aerospace but is also encountered in other domains, such as the biomedical sector [16, 17].

✉ Francesco Lambiase
francesco.lambiase@univaq.it

[1] Department of Industrial and Information Engineering and Economics (DIIIE), University of L'Aquila, Monteluco Di Roio, 67100 L'Aquila, Italy

[2] Monteluco Di Roio, L'Aquila, Italy

Additive manufacturing (AM) processes hold the potential to address the needs for producing low-volume batches, including individual units, of products fabricated from engineering thermoplastics like PEEK [18–20], PAEK [9, 21, 22], and PEI [23–25], with or without fiber reinforcement. Despite these potential advantages, the utilization of AM for the fabrication of critical components in aerospace, as well as in the biomedical field, raises several concerns. These concerns encompass mechanical performance, product repeatability, and material stability, which are paramount among the challenges related to the difficulties in printing these materials. Consequently, comprehensive qualification campaigns are imperative to ensure the performance criteria are met.

Within the spectrum of additive manufacturing (AM) processes, material extrusion (MEX) emerges as a viable candidate for the cost-effective production of aerospace components fabricated from engineering plastics such as PEEK, PAEK, and PEI. MEX facilitates the manufacturing of small- to medium-sized components and, with its relative ease of scalability, presents a potential pathway to produce large-sized components in the foreseeable future. Setting aside the numerous advantages of the MEX process [26–28], a primary challenge associated with this process is the interlayer adhesion [29], which significantly affects the mechanical behavior and anisotropy of the produced components.

Even the tough interlayer adhesion is strongly influenced by the infill strategy and pattern orientation [30–32], the development of interlayer adhesion during the deposition process is due to the entanglement of molecular chains. This phenomenon is promoted by the elevated temperature of the deposited material, which preheats the substrate, thereby enhancing layer adhesion. The mechanism of bonding is thus reliant on the kinetics of the entanglements, which in turn is dependent on the thermal history of the material [33]. Prolonged exposure to higher temperatures is anticipated to foster stronger interlayer adhesion, as it allows molecular chains more time to diffuse between overlapping layers [19, 34–36]. Conversely, during the cooling phase from temperatures exceeding the melting point of semi-crystalline polymers, the formation of crystalline regions may impede the mobility of molecular chains, thereby hindering the interlayer adhesion [12, 35].

Driven by the significant interest from both the aerospace and biomedical sectors in incorporating plastic components constructed from materials such as PEEK, PAEK, and PEI, extensive research efforts have been undertaken to elucidate the mechanical properties of these components [18, 23, 37]. However, the capability to directly fabricate characterization samples through printing has frequently overshadowed, and in some cases even obscured, the potential challenges inherent to this methodology. This method is favored for its simplicity, eliminating the need for additional machining prior to testing. However, this seemingly straightforward practice may give rise to significant issue:

1. Discrepancies in the thermal histories experienced by directly printed samples compared to those encountered by larger components.
2. Potential presence of artifacts resulting from direct printing onto the samples.

The central inquiries addressed in this study are as follows:

1. Can direct printing reliably assess the tensile properties of MEX components fabricated from PAEK along the building direction?
2. What are the principal disparities (and their underlying causes) between the mechanical characteristics of directly printed samples and those of larger components?

In pursuit of uncovering critical insights, an extensive experimental investigation was undertaken to discern and elucidate the differences and potential causal factors that could significantly impact the accurate assessment of the mechanical behavior of PAEK components fabricated via the MEX process. This comprehensive experimental endeavor encompassed a rigorous examination, comprising both directly printed tensile tests and those cut from boxes. The choice of these two manufacturing approaches — direct printing of tensile test samples and extraction from a larger component (the box) — was deliberate and aimed at addressing several key research objectives:

- Representation of real-world scenarios: This dual approach allows us to simulate two common situations in additive manufacturing for aerospace applications. Direct printing represents the production of small components, while the box-cut method mimics the extraction of test specimens from larger parts.
- Thermal history comparison: By using these two strategies, we can investigate the impact of different thermal histories on the material properties. Directly printed samples experience rapid cooling cycles, while samples cut from the box undergo a more gradual cooling process, potentially affecting crystallinity and interlayer adhesion.
- Scale effects: This approach enables us to examine how the scale of the printed part influences the mechanical properties of PAEK components. The thermal gradients and cooling rates in a larger box may differ significantly from those in a small, directly printed sample.
- Manufacturing artifacts: Direct printing of small samples may introduce artifacts due to frequent accelerations and decelerations of the print head. By comparing these with

samples cut from a larger box, we can assess the impact of these artifacts on mechanical properties.
- Interlayer bonding assessment: The two strategies allow us to evaluate how the interlayer bonding strength might differ between small, directly printed parts and larger structures, which is crucial for understanding the overall performance of PAEK components in aerospace applications.
- Porosity and microstructure analysis: By employing these two approaches, we can investigate how the manufacturing strategy affects the internal structure, porosity distribution, and overall material consistency.
- Practical implications: This comparison provides valuable insights for manufacturers and engineers in the aerospace industry, helping them make informed decisions about the most appropriate manufacturing strategy for specific component requirements.

By adopting these two strategies, we aim to provide a comprehensive understanding of how the manufacturing approach influences the mechanical properties, microstructure, and overall performance of PAEK components produced via material extrusion (MEX). This knowledge is crucial for quality assessment of MEX components that is mandatory especially for the production of high-performance aerospace components.

As above mentioned, employing precision abrasive waterjet cutting techniques was pivotal, ensuring meticulous sample preparation without subjecting the edges to thermal cycles. While various conventional (e.g., machining) and unconventional (e.g., laser cutting) processes are available for sample preparation, we specifically chose abrasive waterjet cutting for several critical reasons:

- Thermal neutrality: Unlike machining or laser cutting, which can induce significant thermal cycles, abrasive waterjet cutting is a cold-cutting process. This thermal neutrality is crucial for our study, as it ensures that the mechanical characteristics of the PAEK samples are not altered by heat-induced changes in the material's microstructure or crystallinity during the cutting process.
- Minimal mechanical stress: Waterjet cutting imparts minimal mechanical stress to the workpiece, reducing the risk of introducing residual stresses or micro-cracks that could affect the mechanical properties we aim to measure.
- Clean cut quality: Abrasive waterjet cutting provides a clean, precise cut with minimal burr formation, which is essential for accurate dimensional control and reliable mechanical testing.

All the above advantages led to preservation of material properties; indeed, by avoiding thermal alterations, we ensure that the samples cut from the box maintain their original crystallinity, molecular orientation, and interlayer adhesion characteristics, which are crucial factors in our comparative study.

Notably, some samples underwent annealing, a common post-treatment in aerospace industries to enhance PAEK component properties. The mechanical tests were conducted under quasistatic conditions, with subsequent detailed analyses employing optical and scanning electron microscopy to scrutinize fracture and external surfaces. Moreover, differential scanning calorimetry played a pivotal role, investigating the impact of sample preparation on crystallinity through precise measurements of enthalpy changes during melting and crystallization. These findings hold profound implications, not only for industry practitioners seeking to optimize PAEK component performance but also for the scientific community aiming to refine methodologies for accurate mechanical characterization in advanced manufacturing processes.

2 Materials and methods

2.1 Materials and sample preparation

Polyaryletherketone (PAEK), provided by VICTREX, was utilized for the study, boasting an initial diameter of 1.75 mm ± 0.02 mm. The production of the samples was carried out using an industrial machine model Spectral 30 by 3ntr (from Novara, Italy). The critical deposition parameters, as listed in Table 1, influence the interlayer bonding behavior, surface roughness, and dimensional precision. Key factors, such as nozzle temperature, layer thickness, building plate temperature, extrusion multiplier, infill percentage, and nozzle speed, directly govern the thermal history, thereby influencing interlayer bonding and overall print quality.

Table 1 Main deposition conditions

Process parameter	Value
Printer primary extruder temperature [°C]	398
Printer secondary extruder temperature [°C]	280
Printer plate temperature [°C]	120
Printer chamber temperature [°C]	120
Hotend speed [mm/min]	3600
Nozzle diameter [mm]	0.4
Extrusion width [mm]	0.5
Layer thickness [mm]	0.2
Infill percentage [%]	100
Infill strategy	Linear
Number of perimeter shells	4
Volumetric material flow [mm^3/min]	360

The samples were manufactured according to ASTM D638 [38] standards Type I.

Particularly, the samples were produced using different protocols:

1. Direct printing: the samples were printed at the final dimension;
2. Sample extraction: the samples were cut through abrasive waterjet cutting. To this end, a box with side walls 4 mm of thickness was printed. Then, the samples were cut from the box. Waterjet cutting was used to cut the samples to avoid any material modification since no heating was produced during the cutting operation. This choice was supported by Alberdi [39], who demonstrated the advantages of abrasive waterjet cutting for polymer composites, highlighting its ability to produce high-quality cuts without thermal damage.

This approach allows us to isolate the effects of the manufacturing strategy (direct printing vs. box-cut) on the mechanical properties of the PAEK components, without introducing confounding variables from the sample preparation process itself. Figure 1 presents a detailed schematic of the samples. In both cases, the entire thickness of the sample (of 4 mm) was filled by the external shells. Indeed, each shell was 0.5 mm wide; consequently, at least in the central region, the samples cut from the box and directly printed were produced with the same strategy. Of course, some differences existed in the side regions. Indeed, the cut samples were characterized by filaments arranged along one direction, while directly printed samples showed a concentric shell strategy, as schematized in Fig. 1.

Additionally, some specimens were post-processed by annealing; Fig. 2 shows the thermal cycle that the specimens were subjected during the annealing process. The test matrix of the experimental campaign is summarized in Table 2.

For each processing condition, five samples were produced. Thus, the mean value and standard deviation were computed.

2.2 Samples' characterization

The samples underwent geometrical characterization prior to mechanical testing. The dimensions were measured through microscopy analysis. This enabled to determine the effective cross section (adhesion area) neglecting external defects. Then, the Young's modulus and the tensile strength were calculated accordingly. Tensile tests were performed using a universal testing machine model C43.50 equipped with a 50 kN load cell. The tests were conducted at a traverse

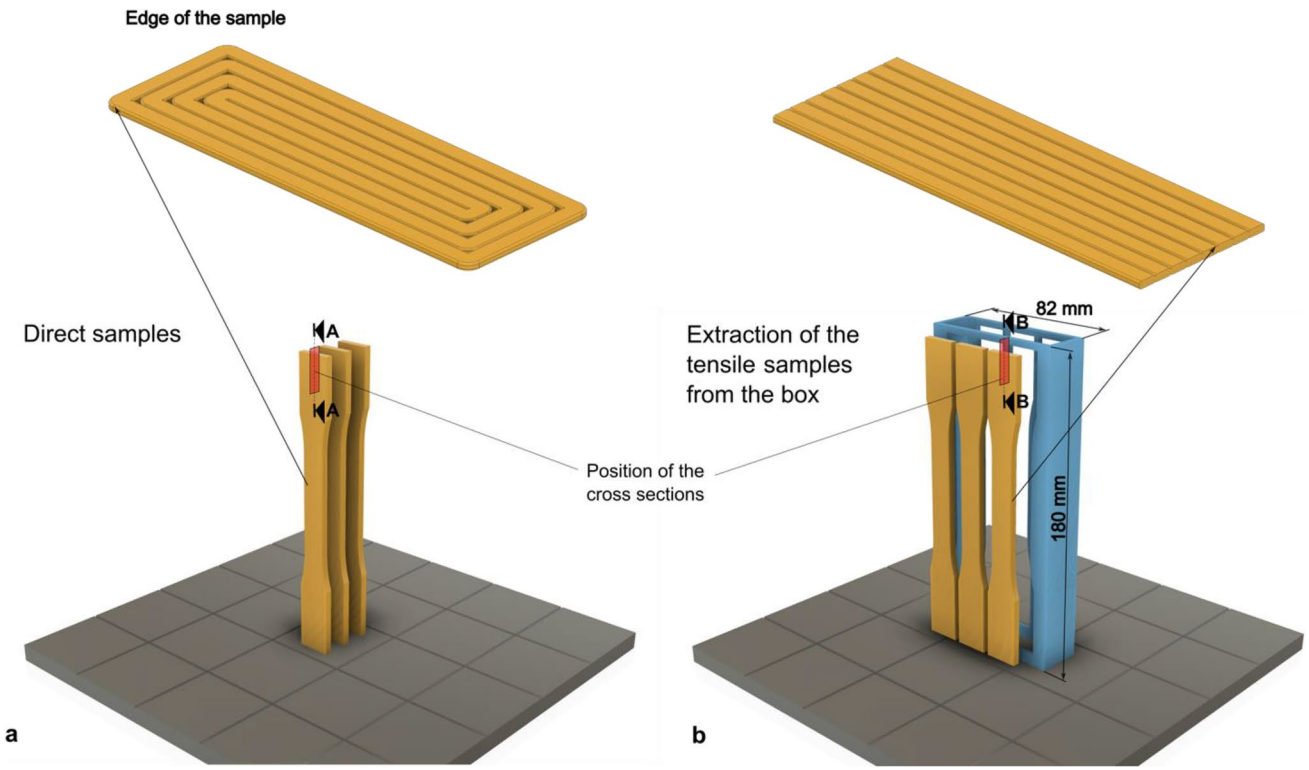

Fig. 1 Schematic of the sample produced using different approaches: **a** direct sample printing, **b** extraction (through abrasive waterjet cutting) of tensile samples from the rectangular box

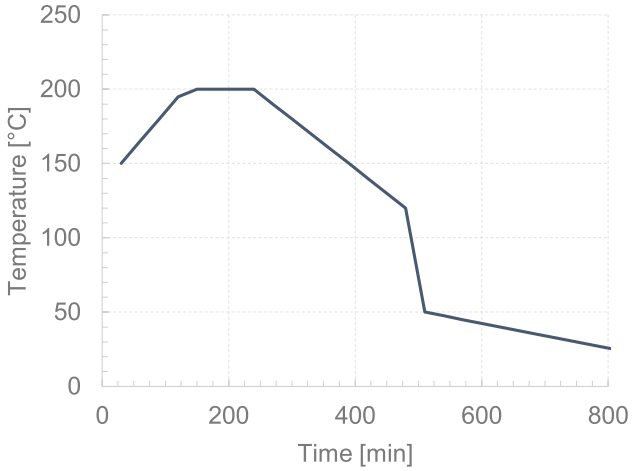

Fig. 2 Annealing thermal cycle

Table 2 Test matrix summarizing the experimental conditions used for the experimental investigation

Manufacturing	Post-processing
Direct print — AP	As printed
Direct print — A	Annealed
Cut from the box — AP	As printed
Cut from the box — A	Annealed

speed of 1 mm/min. During the tests, the strain of the sample was measured using an extensometer model 632.24F-50 by MTS. The tests were carried out until complete failure of the samples. A picture of the sample during the tensile test is presented in Fig. 3.

Optical microscopy served as a valuable tool in understanding the material's morphology both pre- and post-mechanical tests. To this end, a stereoscope model M205 by LEICA was used to determine the real dimension of the cross section, the surface morphology, and the analysis of the fracture surface.

Calorimetric analyses were conducted by differential scanning calorimetry (Perkin Elmer DSC 8500) with 20 °C/min heating/cooling rate. Heating was conducted from 25 to 350 °C.

Crystallinity ratio χ was determined for all the samples from the melting enthalpy ΔH_m according to Eq. 1.

$$\chi(\%) = \frac{\Delta H_m - \Delta H_{cc}}{\Delta H_\infty} \quad (1)$$

where ΔH_{cc} is the cold crystallization enthalpy and ΔH_∞ is the theoretical melting enthalpy of a 100% crystalline polymer. To this end, the ΔH_∞ for PEEK was used which equals 130 J g^{-1} [40].

Fig. 3 Picture of the sample during the tensile test with extensometer

3 Results

3.1 Mechanical behavior

After the tensile tests, fractures typically occurred at the middle of the samples, although there were a few exceptions, particularly among some directly printed samples. Conversely, all the cut samples fractured at the middle of the narrow region. Figure 4 shows some examples of the specimens. Depending on the adopted sample preparation protocol, the samples exhibited different colors.

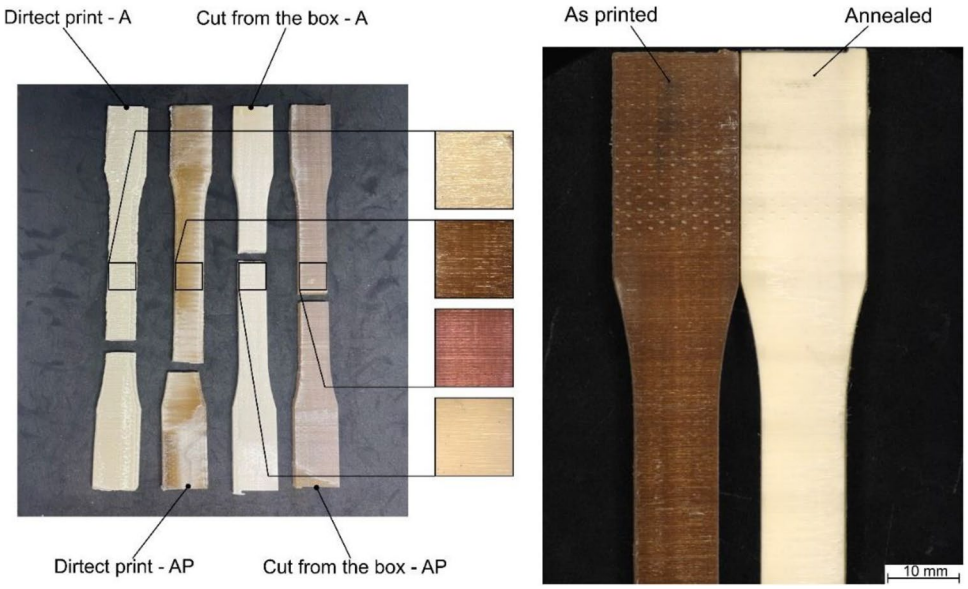

Fig. 4 Pictures of samples produced according to ASTM D638 Type I

After annealing, regardless of the production strategy, the samples displayed an opaque beige color, indicating the development of crystalline structures. In contrast, the samples cut from the box under the "as printed" condition exhibited a translucent brown color, suggesting that the material was mainly in an amorphous state. Directly printed samples showed higher opacity and a lighter color, potentially indicating the onset of crystallization during printing.

Figure 5 shows the side view of the samples from which it is evident the different morphology of the samples in correspondence of the edges. Indeed, directly printed samples showed an irrelugar shape (typical of the MEX process) while the samples cut from the box showed a more regular flat surface.

Figure 6 illustrates the stress–strain curves obtained from the tensile tests conducted using various sample manufacturing methods. Each curve exhibits an initial nearly linear rise in stress associated with the elastic region, followed by a peak load, and then a plateau, signifying the initiation of plastic deformation. In samples fabricated through direct printing, the load abruptly dropped to zero after minimal plastic deformation, resulting in brittle failure. Conversely, specimens cut from the box displayed a prolonged plastic deformation zone, characterized by significantly higher elongation at rupture.

The main mechanical characteristics were identified from the stress–strain curves, including the Young's modulus, the elongation at rupture, and the peak strength. This enabled a deeper comparison among the samples produced with different protocols. Figure 7a compares the Young's modulus. All the samples (except those cut from box under as-printed conditions) exhibited a similar Young's modulus (with average value of 2.66 GPa), irrespective of the manufacturing conditions.

Figure 7b indicates that a more marked difference among the specimen manufacturing strategy is noticeable when considering the peak stress. Direct printed samples showed a peak stress of almost 31 MPa, which was lower than that of cut samples which was 69 MPa (for annealed cut samples) and 60 MPa (for cut samples "as printed"). Furthermore, the tensile strength of directly printed samples suffered from higher dispersion while that of samples cut from box was much more repetitive. Figure 7c compares the elongation at rupture ε_{max}; even for the elongation at rupture, there is a remarkable difference between specimen produced with direct printing and cut from the box. Direct printed samples showed a peak of ε_{max} of about 2%; cut samples, on the other hand, showed higher elongation at rupture and its value is more influenced by annealing post-treatment. For samples cut from the box, annealed samples showed an average elongation at rupture of almost 6%, while as-printed samples showed a value of 8%. This further confirms that substantial differences between as-printed and annealed samples only occurred on cut samples, while negligible differences were observed in directly printed samples.

3.2 Optical analysis

Optical analysis based on cross section analysis and fracture surface analysis were performed to understand the influence of the sample manufacturing strategy on the failure modes. Figure 7 depicts the cross sections of two samples extracted from the positions indicated in Fig. 1 produced through direct print (Fig. 7a) and cut from box (Fig. 7b). As can be inferred, profound differences exist between these

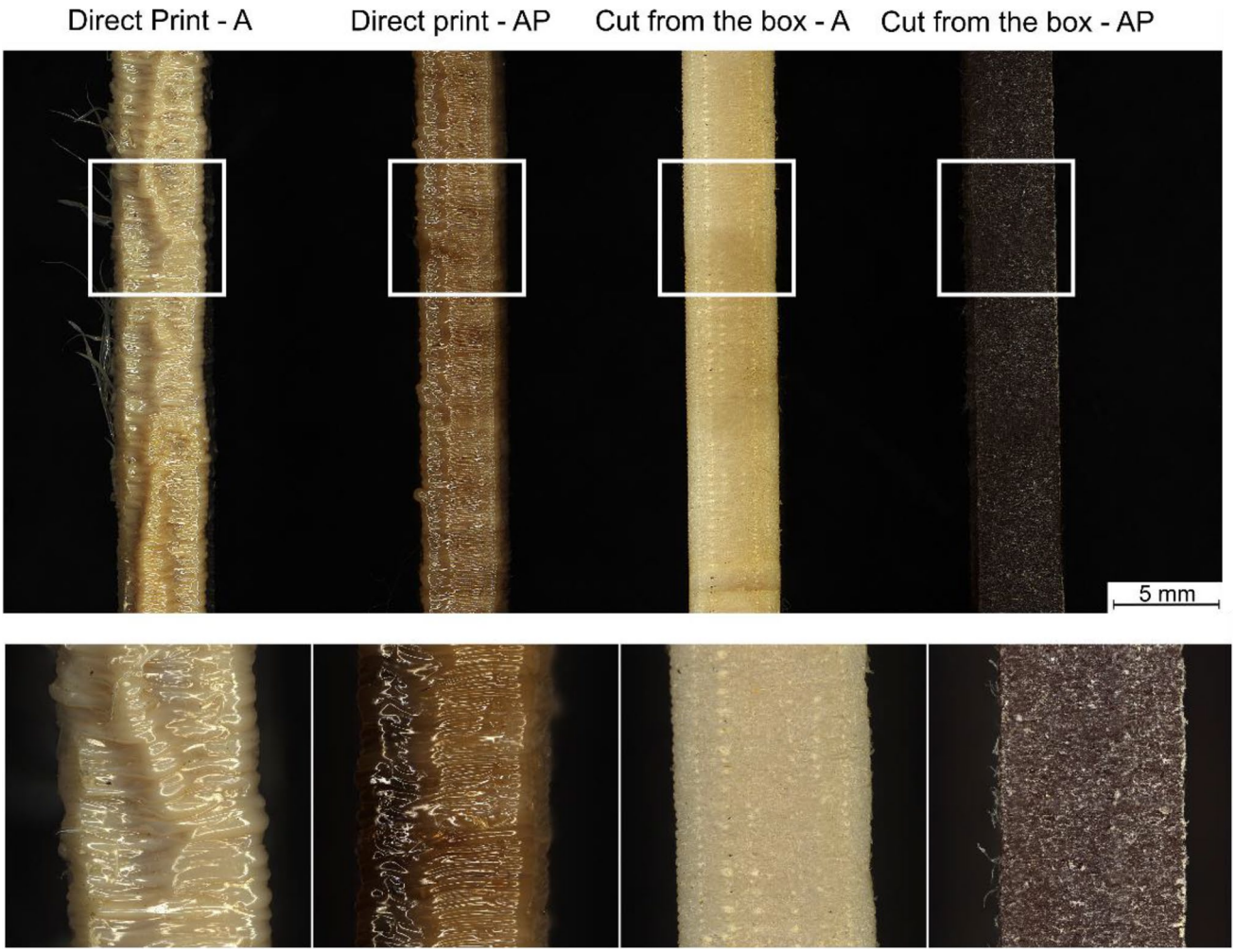

Fig. 5 Side view of the samples at low and higher magnifications

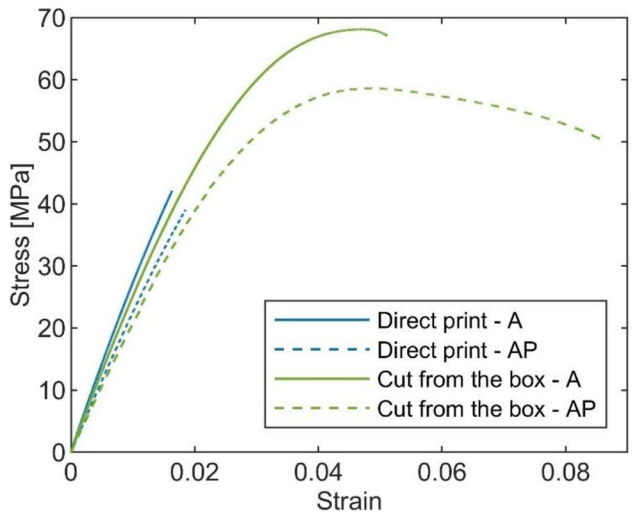

Fig. 6 Stress–strain curves of different samples produced with direct sample printing and cutting one

samples since directly printed samples show fewer porosities unevenly distributed, while the cross section in Fig. 7b indicates a higher number of porosities distributed in a more regular pattern on the sample cut from the box.

The fracture surfaces of the samples after tensile tests were analyzed: directly printed samples failed by interlayer delamination (irrespective of being under "as-printed" or "annealed" state). This failure mode was also observed in cut samples under as-printed condition. On the other hand, cut samples under annealing condition failed by intralayer fracture, as shown in Fig. 8a. This failure mode is indicative of a much stronger adhesion between the layers achieved through the annealing post-process. Indeed, the adhesion between consecutive layers was found to be so robust that a crack caused the fracture of several filaments within the same layer. Conversely, delamination, referring to the separation between consecutive layers, demonstrated the failure in the bond strength between these layers. The occurrence of delamination suggests a relatively weaker adhesion resulting

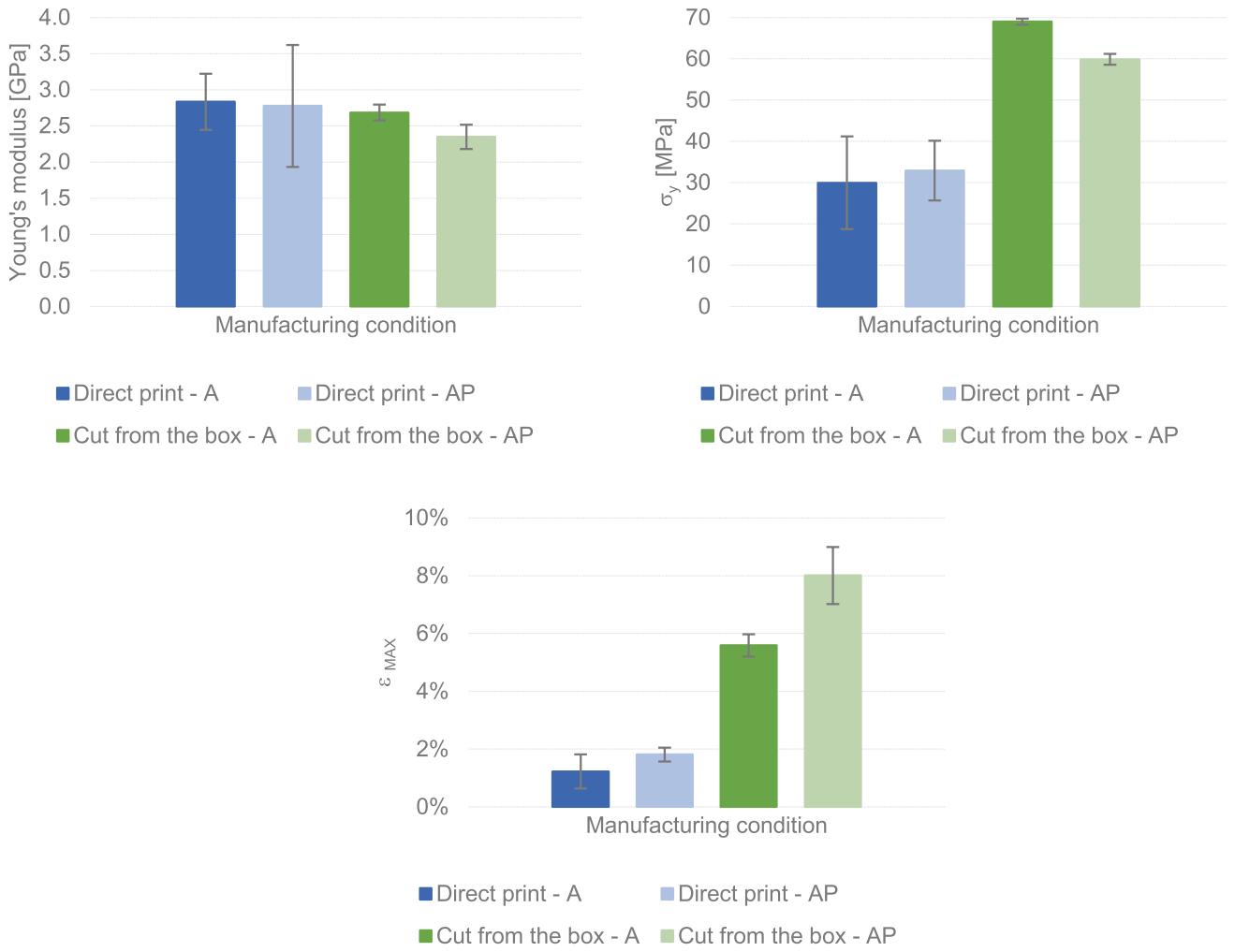

Fig. 7 Mechanical characteristics of the samples produced using different manufacturing strategies

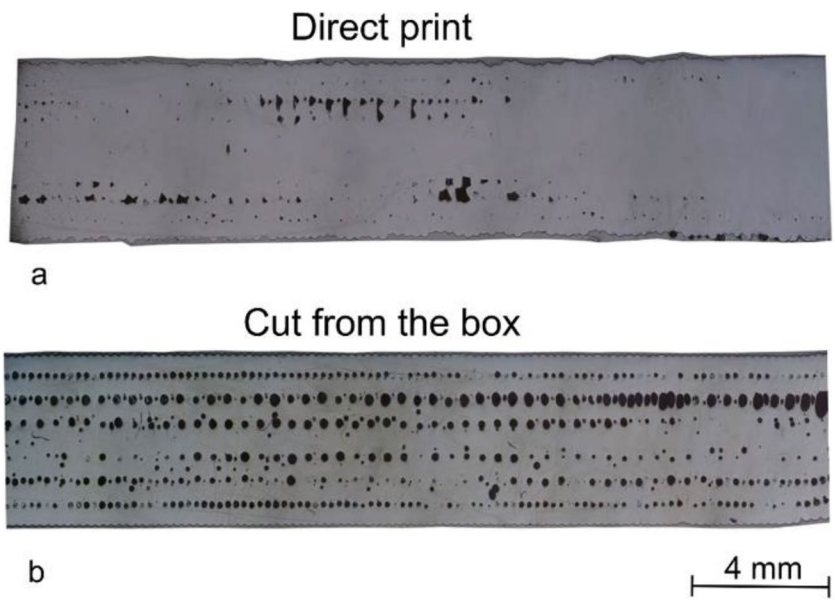

Fig. 8 Cross section of **a** directly printed sample and **b** cut sample. (SECT. AA—direct print and SECT. BB—cut from the box)

from the material extrusion (MEX) process, in comparison to fractures occurring within the filaments themselves Fig. 9.

3.3 Geometrical artifacts

During the deposition of relatively small features (as compared to the nozzle diameter), some geometrical artifacts can develop. The main cause is the acceleration/deceleration regions that occur at the directly printed samples' edges. Indeed, at the edge, the extruder change in direction leads to an acceleration up to the selected printing speed from zero. Similarly, as the extruder approaches to the edges, it decelerates from the set speed to zero. Within acceleration and deceleration ramp regions, uneven material flow is produced since the difficulty (for the MEX machine) to precisely control the material feeding under such speed gradients. This is also due the low viscosity of the material and pressure variations within and underlying the nozzle, which makes very complex the material flow control under unsteady deposition conditions. Figure 10a depicts a 3D view in false colors of a fractured cross section of a directly printed sample. As can be noted, the fracture surface morphology indicates a different adhesion from the left side (where a smoother surface is observable) from the right side where a more fragmented surface is shown. This indicates an uneven adhesion within the sample. On the other hand, Fig. 10b shows the fracture surface of a cut sample (after annealing). Here, the picture shows a

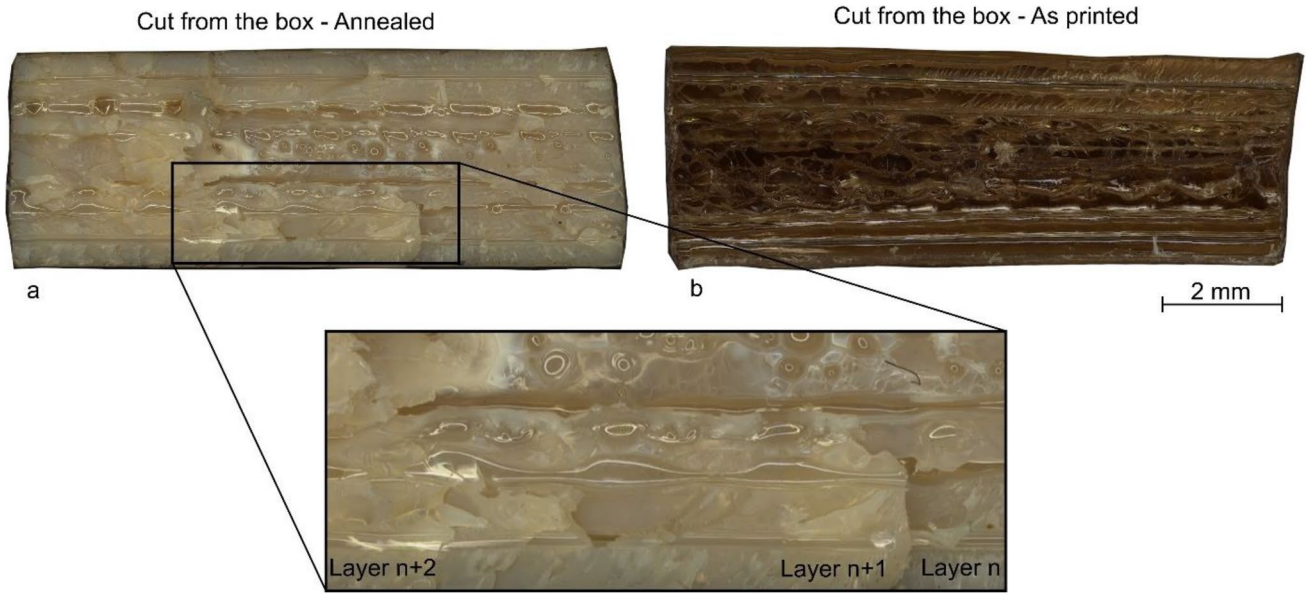

Fig. 9 Fracture surfaces of cut samples under **a** annealing and **b** as-printed conditions

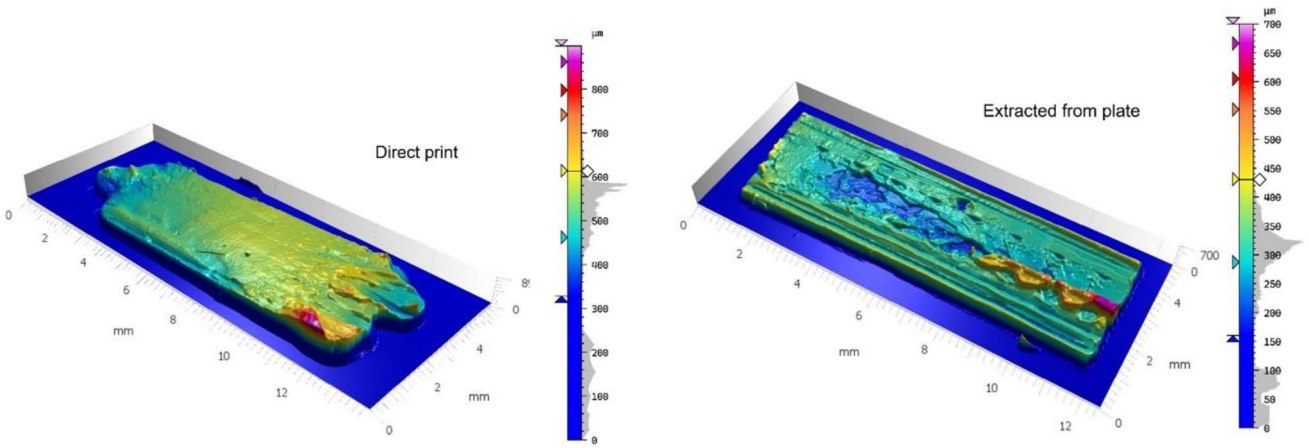

Fig. 10 3D analysis of the fracture surfaces showing **a** directly printed sample and **b** cut sample both under "as-printed condition"

more regular (and rectangular) shape and more homogeneous conditions of adhesion.

More precise observations of the fracture surfaces were conducted using Scanning Electron Microscopy (SEM). As depicted in Fig. 10a, the fracture surface of a directly printed sample tested after the annealing post-process exhibits an almost monolithic appearance, indicating robust adhesion between paths within the same layer. This was due to the relatively short interlayer time that increased the adhesion of paths within the same layer. However, the surface appears relatively smooth, confirming the comparatively weak interlayer bonding that resulted in delamination of the sample (owing to the incipient crystallization). In contrast, Fig. 10b displays the fracture surface of a sample cut from the box following the annealing post-treatment. The morphology of this fracture surface markedly differs, characterized by a highly fragmented appearance and intralayer fractures. This disparity underscores the significant differences in material deposition between directly printed samples and those obtained via cutting from the box Fig. 11.

The 3D reconstruction of the surface of the samples, as reported in Fig. 12, also indicates a more repeatable surface on samples cut from box as compared to directly printed samples. This represents a key difference also in terms of repeatability. Indeed, the presence of a more consistent surface (as that of cut samples) led to higher repeatability of the mechanical characteristics of the samples (smaller standard deviations). On the other hand, the presence of deep and localized grooves in the directly printed samples represented natural regions where stress concentration can develop. These defects can explain the lower tensile strength and elongation at rupture exhibited by directly printed samples as compared to cut ones. Figure 12 also depicts the virtual cross section views that further indicate the profound differences between the surfaces. Indeed, the surface of the directly printed samples

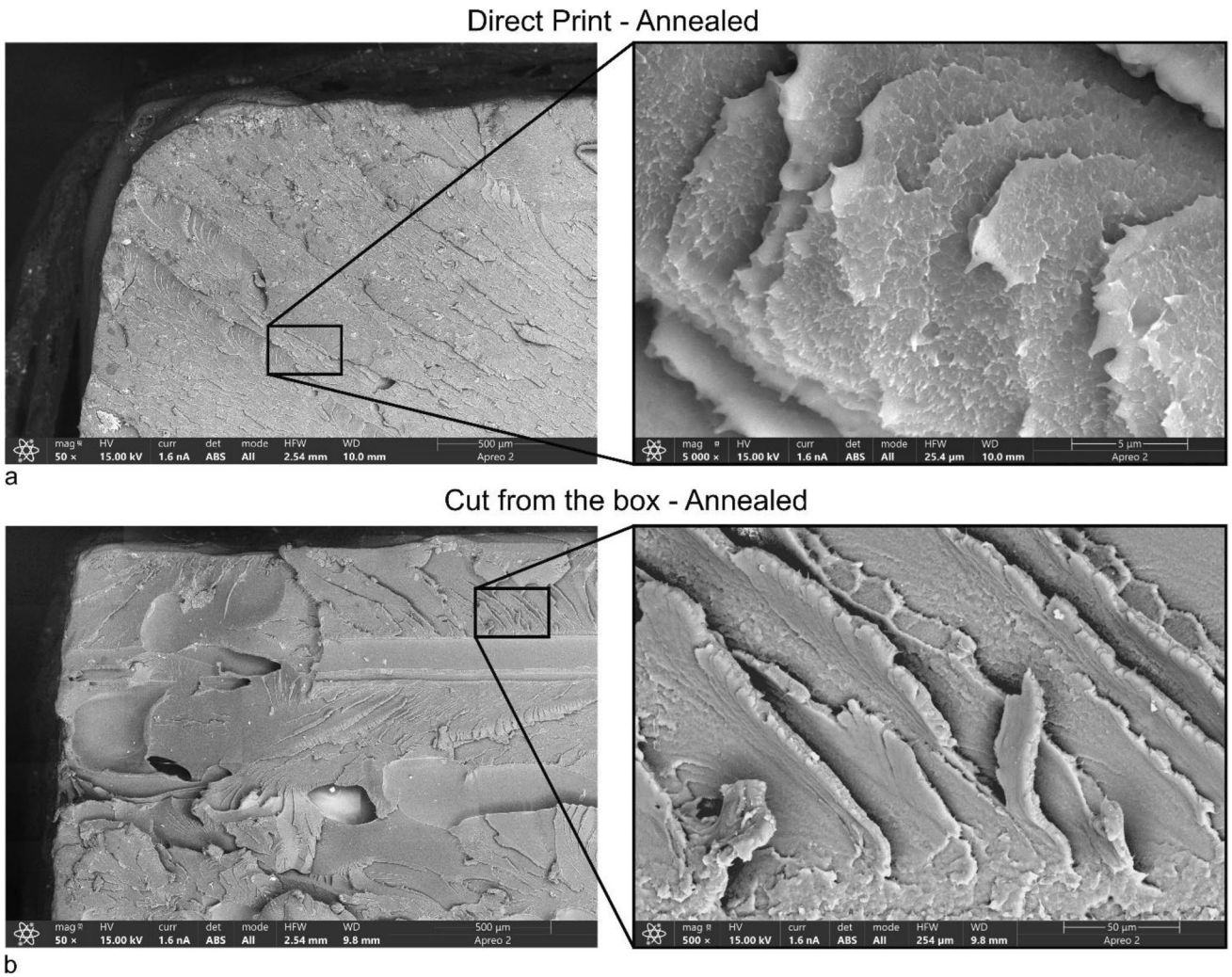

Fig. 11 Fracture surfaces observed through SEM of **a** directly printed and **b** cut from the box samples both after annealing posttreatment

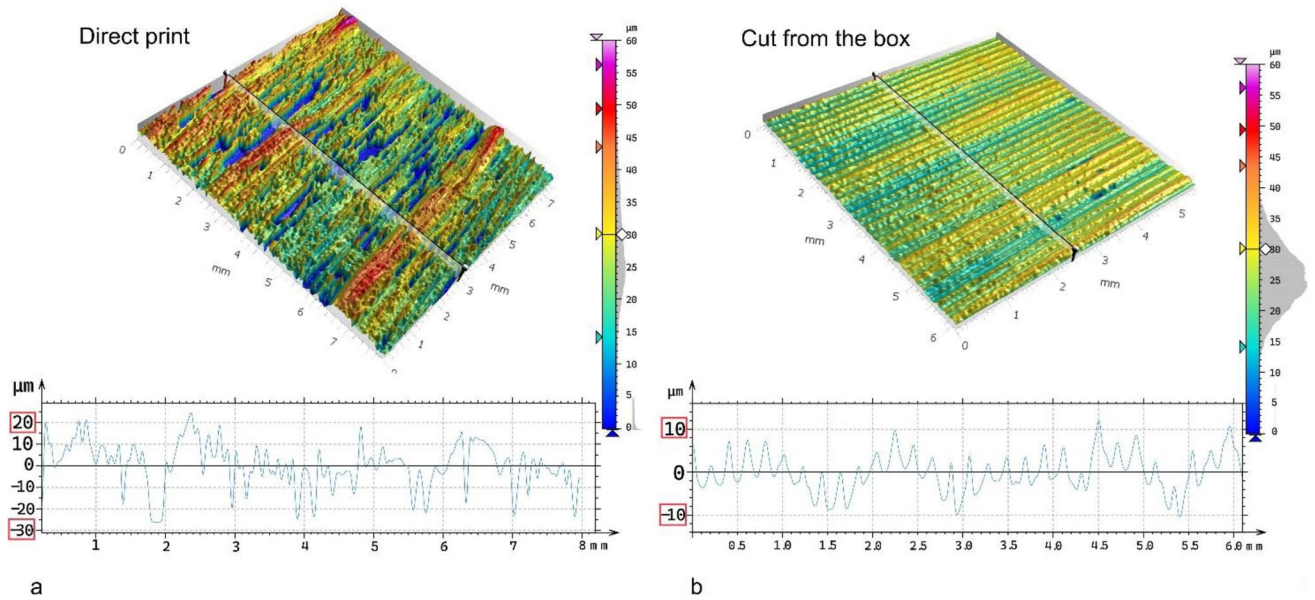

Fig. 12 3D reconstruction of the samples surface produced by different methods: **a** direct print and **b** cut from the box

is characterized by randomly positioned grooves which are deeper (up to 26 µm); on the other hand, the surface of the cut samples is more regular with less deep grooves (up to 10 µm).

The worser surface of directly printed samples can be ascribed to the above-mentioned acceleration-deceleration regions. Besides, a higher substrate temperature (owing to smaller layer) can also provide lower material flow control since the substrate is still under rubbery state during the deposition of the overlying layer. This could be a further cause geometrical artifacts that affect the directly printed samples.

3.4 DSC analysis

To examine the characteristics of the samples produced with different strategies, differential scanning calorimetry tests were performed on all the samples. Figure 13 depicts the DSC results for samples directly printed and cut from box under as-printed and annealed states. The melting enthalpies and the cold crystallization enthalpies were calculated for each condition to determine the crystallization percentages, which are summarized in Table 3.

As can be inferred, the percentage of crystallinity of the samples cut from the box under "as-printed" condition was 3.27%; such value was much smaller than that achieved after

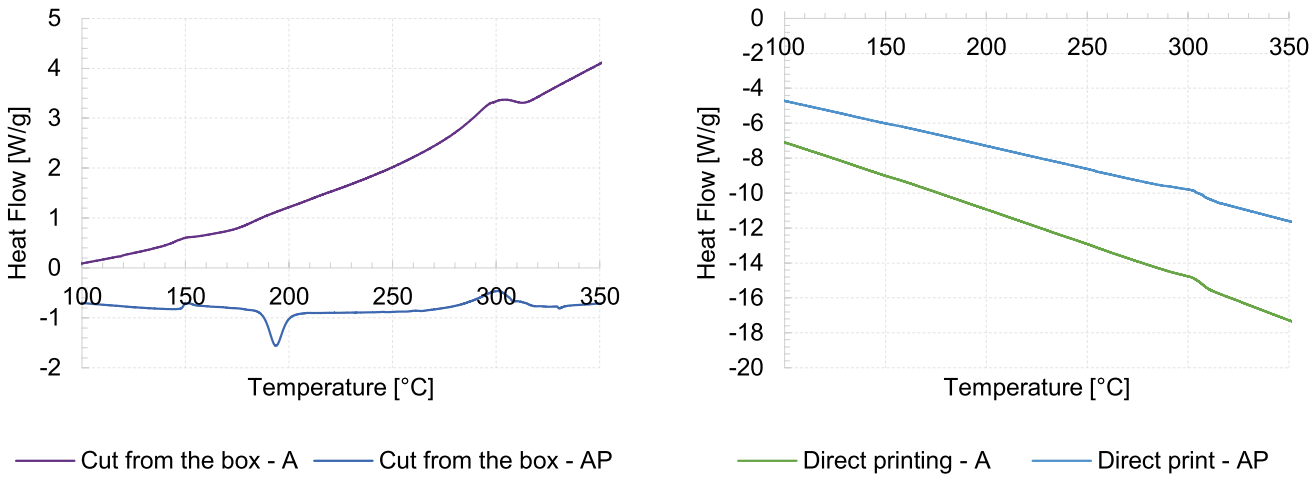

Fig. 13 DSC curves of the samples produced through different deposition and post-process conditions

Table 3 Measurement of enthalpies and crystallinity of the samples produced through different deposition and post-process conditions

Manufacturing condition	ΔH_{Cryst} [J/g]	ΔH_{Melt} [J/g]	χ [%]
Direct print — as printed	-	15.01	11.55
Direct print — annealed	-	15.11	11.62
Cut from the box — as-printed	− 16.66	20.91	3.27
Cut from the box — annealed	-	15.31	11.77

the annealing post-treatment (11.77%). These values confirm the almost amorphous nature of the as-printed samples cut from the box and the increase in the crystallization after the annealing process. On the other hand, the directly printed samples under "as-printed" condition showed a much higher percentage of crystallinity (12.18%). This confirms the onset of an incipient crystallization achieved during the deposition process owing to the smaller layer dimension which led to shorter interlayer time and higher substrate temperature. This promoted the crystallization observed on the directly printed samples under "as-printed" conditions.

4 Discussion

4.1 Key results

The findings of this study shed light on the critical factors influencing the mechanical behavior and crystallinity of material extrusion (MEX) process components fabricated with polyaryletherketone (PAEK). Through the comparison of two sample preparation methods, direct printing and samples cut from a box, along with annealing treatments, significant differences in mechanical properties and crystallinity were observed. The main differences between directly printed samples and cut from the box included deposition and filling conditions, formation of crystalline region during material deposition, external surface morphology, mechanical behavior, fracture mode, and influence of post-treatments.

The main causes of such discrepancies were:

- Directly printed samples showed uneven deposition patterns owing to frequent accelerations/decelerations which also led to lower material flow control during the deposition. These irregular (uncontrolled) material depositions were present on directly printed sample, while they were avoided in samples cut from the box;
- Different thermal history owing to a different dimension of the layer.

This highlights the importance of understanding the thermal history experienced during the printing process. Directly printed samples exhibited lower tensile strength and elongation at rupture compared to samples extracted from a box. A marginally influenced Young's modulus suggests that the processing conditions primarily affect the adhesion of subsequent layers rather than the overall stiffness of the material. However, the analysis of the fracture surfaces underscores significant differences also in terms of deposition patterns.

The reduced tensile strength of directly printed samples, corresponding to approximately 50% of the strength of cut samples, can be attributed to the presence of artifacts resulting from continuous accelerations/deceleration of the hotend along the sample cross section. In addition, the different thermal history experienced between direct printing and printing a larger box involved a higher degree of crystallinity in the directly printed samples. This limited the polymeric chains' entanglement through the layers and consequently the elongation at rupture and the tensile strength. The observed difference in crystallinity further supports the influence of processing conditions on the material properties. Directly printed samples exhibited a higher degree of incipient crystallization compared to samples extracted from a box. This suggests that the thermal gradients and cooling rates experienced during direct printing promote the formation of crystalline structures within the material. In contrast, samples cut from a box were affected by a lower amount of crystallinity.

The key point of the paper lies in the potential discrepancies between the mechanical properties of directly printed test samples and those of larger components in real-world applications, particularly in industries like aerospace where such discrepancies can have critical implications. Many industries, including aerospace, commonly use direct sample printing for quality assessment of mechanical properties, which are then used in simulations and design of larger components. This study demonstrates how significantly different these mechanical characteristics can be, due to several factors:

- Thermal history: The thermal cycles experienced during printing differ significantly between small, directly printed samples and larger components. This variation affects the degree of crystallinity, which in turn influences the entanglement of polymeric chains between layers during deposition, ultimately impacting mechanical behavior.
- Flow dynamics: The presence of perimetral shells in directly printed samples indeed influences local deposition flow. The extruder undergoes steep accelerations/decelerations at the edges, altering the thermal cycle and local pressure. These factors contribute to the differences in mechanical properties we observed.
- Scale effects: The size difference between directly printed samples and the larger box from which samples are cut

leads to different cooling rates and thermal gradients, further influencing the material's microstructure and properties.

Mechanical characterization tests should accurately reflect the material behavior of real components. Our results demonstrate that for PAEK components manufactured via material extrusion (MEX), the sample preparation method significantly influences the measured mechanical properties. This finding highlights the critical importance of choosing appropriate testing methodologies that align with the intended application and component scale. This research serves as a cautionary note to industries relying on directly printed test samples. It highlights the potential risks of using data from such samples to predict the behavior of larger, more complex components. By quantifying these differences, we provide valuable insights that can lead to more accurate testing methodologies and improved design processes for PAEK components in critical applications like aerospace.

4.2 Limitations and generalizability

The main limitation of the study and the generalizability of the results are summarized as follows:

- Material specificity: While our results on PAEK can be expected to apply to other thermoplastics, particularly semicrystalline materials, the magnitude of the observed differences may vary. Recent studies by our team on polylactide acid (PLA) in tensile [41] and compression tests [42] showed similar trends, but the differences between directly printed and box-cut samples were more pronounced in PAEK. This indicates that these effects are strongly influenced by both the material properties and deposition conditions.
- Test methodology: Our study focused on tensile testing. While this provides valuable insights, it does not capture the full range of mechanical properties relevant to aerospace applications. Additional characterization methods such as interlayer compression, bending tests, fracture toughness, and impact testing could provide a more comprehensive understanding of the differences between manufacturing strategies.
- Sample geometry constraints: The interlayer time, which significantly influences thermal history, interlayer adhesion, and crystallization degree, is heavily dependent on the sample cross-section perpendicular to the building direction. This makes it challenging to produce samples conforming to different testing standards (tension, compression, bending, fracture toughness) with identical thermal histories, potentially limiting the comparability of results across different test types.

5 Future prospects

The main future perspectives of the study are summarized as follows:

- Expanded testing: Future studies will aim to extend the experimental characterization procedure to include additional mechanical tests, providing a more comprehensive understanding of how manufacturing strategy affects various mechanical properties.
- Material range: We plan to investigate whether these findings extend to other high-performance thermoplastics used in aerospace applications, such as PEEK, PEI, or PEKK.
- Process parameter optimization: Further research could focus on optimizing printing parameters to minimize the differences between directly printed samples and larger components, potentially improving the reliability of small-scale testing for predicting large-component behavior.
- In situ monitoring: Development of in situ monitoring techniques during printing could provide valuable insights into the real-time development of material properties and help explain the observed differences.

6 Conclusions

The study proved the strong relevance of the manufacturing strategy of tensile tests of components made by material extrusion (MEX) process of PAEK for aerospace industry. Two testing strategies were investigated: direct sample printing and samples cut from a printed box. This second solution is representative of larger components (as compared to small cross sections of the tensile samples). The main results from the research are summarized as follows:

- The Young's modulus was poorly influenced by the manufacturing strategy and adoption of annealing after the material extrusion;
- Directly printed samples required shorter interlayer time. This involved higher substrate temperature which led to lower cooling rates, deposition over rubbery state material (lower material flow control), and higher degree of crystallinity, which inhibited polymerics chain entanglement leading to weaker adhesion. This led to lower tensile strength and elongation at rupture (30 MPa and 2%, respectively) of directly printed samples as compared to samples extracted from the box (60 MPa and 8%, respectively).

- The tensile strength of directly printed samples after annealing (average of 30 MPa) was like that of samples without annealing. This was due to the incipient crystallization achieved during deposition and production of directly printed samples. On the other hand, the tensile strength of the samples cut from the box after annealing was 69 MPa indicating a further increase in the mechanical properties after annealing.
- The analysis of fracture surfaces revealed notable artifacts in directly printed samples compared to those cut from the box. This underscores the necessity to avoid directly printed samples for tensile tests of materials produced by the MEX process, as their behavior may significantly diverge from that of actual components.

Acknowledgements The authors would like to greatly acknowledge Mr. Giuseppe Spagnoli from DIIIE—UNIVAQ for his contribution to DSC tests and Doct. Lorenzo Arrizza from Microscopy Center of UNIVAQ from Scanning Electron Analysis and Eng. Fabrizio Poscente and Eng. Daniele Martinazzo from Thales for making the specimens.

Author contribution F.L. and A.P.: supervision. F.L., A.P., SI. S., and F.P.: conceptualization methodology. F.L.: data curation. F.L., SI. S., A.P., and F.P.: writing — original draft, writing.

Funding Open access funding provided by Università degli Studi dell'Aquila within the CRUI-CARE Agreement. This research was conducted within the project: "OCEANOS—Monitoraggio coltivazioni e zone marine costiere: Tecnologie satellitari di nuova generazione" — ARS01_00536.

Data availability The data supporting this study's findings are available from the corresponding author, Francesco Lambiase, upon reasonable request.

Declarations

Competing interest The authors declare no competing interests.

References

1. Shekar RI, Kotresh TM, Rao PMD, Kumar K (2009) Properties of high modulus PEEK yarns for aerospace applications. J Appl Polym Sci 112(4):2497–2510
2. Vakharia VS, Leonard H, Singh M, Halbig MC (2023) Multi-material additive manufacturing of high temperature polyetherimide (PEI)-based polymer systems for lightweight aerospace applications. Polymers (Basel) 15(3):561
3. Wang P, Zou B, Ding S, Li L, Huang C (2021) Effects of FDM-3D printing parameters on mechanical properties and microstructure of CF/PEEK and GF/PEEK. Chin J Aeronaut 34(9):236–246
4. Abdullah F, Okuyama K-I, Morimitsu A, Yamagata N (2020) Effects of thermal cycle and ultraviolet radiation on 3D printed carbon fiber/polyether ether ketone ablator. Aerospace 7(7):95
5. Hopping EP, Huang W, Xu KG (2021) Small hall effect thruster with 3d printed discharge channel: design and thrust measurements. Aerospace 8(8):227
6. Kalra S, Munjal BS, Singh VR, Mahajan M, Bhattacharya B (2019) Investigations on the suitability of PEEK material under space environment conditions and its application in a parabolic space antenna. Adv Space Res 63(12):4039–4045
7. Dua R, Rashad Z, Spears J, Dunn G, Maxwell M (2021) Applications of 3D-Printed PEEK via Fused Filament Fabrication: a systematic review. Polymers. https://doi.org/10.3390/polym13224046
8. Das A, Chatham CA, Fallon JJ, Zawaski CE, Gilmer EL, Williams CB, Bortner MJ (2020) Current understanding and challenges in high temperature additive manufacturing of engineering thermoplastic polymers. Addit Manuf 34:101218
9. Arquier R, Iliopoulos I, Régnier G, Miquelard-Garnier G (2022) Consolidation of continuous-carbon-fiber-reinforced PAEK composites: a review, Materials Today Communications 32. https://doi.org/10.1016/j.mtcomm.2022.104036
10. Gómez-García D, Díaz-Álvarez A, Youssef G, Miguélez H, Díaz-Álvarez J (2023) Machinability of 3D printed peek reinforced with short carbon fiber, Composites Part C: Open Access 12. https://doi.org/10.1016/j.jcomc.2023.100387
11. Ji Y, Luan C, Yao X, Ding Z, Niu C, Dong N, Fu J (2023) Mechanism and behavior of laser irradiation on carbon fiber reinforced polyetheretherketone (CF/PEEK) during the laser-assisted in-situ consolidation additive manufacturing process. Addit Manuf 74:103713
12 Rodzeń K, Harkin-Jones E, Wegrzyn M, Sharma PK, Zhigunov A (2021) Improvement of the layer-layer adhesion in FFF 3D printed PEEK/carbon fibre composites. Compo Part A: Appl Sci Manuf 149:106532
13 Hanemann T, Klein A, Baumgärtner S, Jung J, Wilhelm D (2023) Material Extrusion 3D Printing of PEEK-Based Composites. Polymers 15:3412
14 Rodzen K, McIvor MJ, Sharma PK, Acheson JG, McIlhagger A, Mokhtari M, McFerran A, Ward J, Meenan BJ, Boyd AR (2021) The Surface Characterisation of Fused Filament Fabricated (FFF) 3D Printed PEEK/Hydroxyapatite Composites. Polymers (Basel) 13(18):3117
15. Rodzen K, Sharma PK, McIlhagger A, Mokhtari M, Dave F, Tormey D, Scherlock R, Meenan BJ, Boyd A (2021) The direct 3D printing of functional PEEK/hydroxyapatite composites via a fused filament fabrication approach. Polymers 13:545
16. Najeeb S, Zafar MS, Khurshid Z, Siddiqui F (2016) Applications of polyetheretherketone (PEEK) in oral implantology and prosthodontics. J Prosthodont Res 60(1):12–19
17. Oladapo BI, Zahedi SA, Ismail SO, Omigbodun FT (2021) 3D printing of PEEK and its composite to increase biointerfaces as a biomedical material- A review. Colloids Surf B Biointerfaces 203:111726
18. Arif MF, Kumar S, Varadarajan KM, Cantwell WJ (2018) Performance of biocompatible PEEK processed by fused deposition additive manufacturing. Mater Des 146:249–259
19. Basgul C, MacDonald DW, Siskey R, Kurtz SM (2020) Thermal localization improves the interlayer adhesion and structural integrity of 3D printed PEEK lumbar spinal cages. Materialia (Oxf) 10:100650

20 Deng X, Zeng Z, Peng B, Yan S, Ke W (2018) Mechanical Properties Optimization of Poly-Ether-Ether-Ketone via Fused Deposition Modeling. Materials (Basel) 11(2):216

21 Marathe U, Padhan M, Panier S, Bijwe J (2021) Processing of PAEK-graphite fabric composites – Pros and cons of film technique over powder sprinkling technique. Compos Part B: Eng 215:108804

22. Yi N, Davies R, Chaplin A, McCutchion P, Ghita O (2021) Slow and fast crystallising poly aryl ether ketones (PAEKs) in 3D printing: Crystallisation kinetics, morphology, and mechanical properties. Addit Manuf 39:101843

23. Gebisa AW, Lemu HG (2019) Influence of 3D Printing FDM Process Parameters on Tensile property of ULTEM 9085. Procedia Manuf 30:331

24. Byberg KI, Gebisa AW, Lemu HG (2018) Mechanical properties of ULTEM 9085 material processed by fused deposition modeling. Polym Testing 72:335–347

25. Volkov YM, Vorobev EV, Drozdov AV, Zemtsov MP, Novogrudskii LS, Kanivets IA, Kharchenko VM (2020) Effect of a Temperature on the Mechanical Characteristics of ULTEM 9085 Thermoplastic Produced by Additive Technology. Strength of Materials 52(3):414

26. Durão LFC, Christ A, Anderl R, Schützer K, Zancul E (2016) Distributed manufacturing of spare parts based on additive manufacturing: use cases and technical aspects. Procedia CIRP 57:704–709

27. Perez-Mañanes R, Garcia-de San José S, Desco-Menéndez M, Sánchez-Arcilla I, González-Fernández E, Vaquero-Martín J, González-Garzón JP, Mediavilla-Santos L, Trapero-Moreno D, Calvo-Haro JA (2021) Application of 3D printing and distributed manufacturing during the first-wave of COVID-19 pandemic. Our experience at a third-level university hospital, 3D Printing in Medicine 7:1–8. https://doi.org/10.1186/s41205-021-00097-6

28. Wittbrodt BT, Glover AG, Laureto J, Anzalone G, Oppliger D, Irwin J, Pearce JM (2013) Life-cycle economic analysis of distributed manufacturing with open-source 3-D printers. Mechatronics 23(6):713–726

29. Lambiase F, Liparoti S, Pace F, Scipioni SI, Paoletti A (2024) A multidisciplinary approach to investigate the influence of process parameters on interlayer adhesion in material extrusion additive manufacturing. Int J Adv Manuf Technol 133:5553–5570

30. Lambiase F, Stamopoulos AG, Pace F, Paoletti A (2023) Influence of the deposition pattern on the interlayer fracture toughness of FDM components. Int J Adv Manuf Technol 128(9–10):4269–4281

31. Fountas NA, Papantoniou I, Kechagias JD, Manolakos DE, Vaxevanidis NM (2024) Experimental and statistical investigation on flexural properties of FDM fabricated PLA specimens applying response surface methodology. J Phys: Conf Ser 2692(2024):012047

32. Kechagias J, Zaoutsos S (2024) Effects of 3D-printing processing parameters on FFF parts' porosity: outlook and trends. Mater Manuf Processes 39(6):804–814

33. Lee A, Wynn M, Quigley L, Salviato M, Zobeiry N (2022) Effect of temperature history during additive manufacturing on crystalline morphology of PEEK. Adv Ind Manuf Eng 4:100085

34. Shelton TE, Willburn ZA, Hartsfield CR, Cobb GR, Cerri JT, Kemnitz RA (2020) Effects of thermal process parameters on mechanical interlayer strength for additively manufactured Ultem 9085. Polym Testing 81:106255

35. Lepoivre A, Boyard N, Levy A, Sobotka V (2020) Heat Transfer and adhesion study for the FFF additive manufacturing process. Procedia Manuf 47:948

36. Lambiase F, Pace F, Andreucci E, Paoletti A (2024) The effect of the interlayer time and deposition speed on the tensile properties of material extrusion components. Int J Adv Manuf Technol 133:6111–6121

37. Algarni M, Ghazali S (2021) Comparative study of the sensitivity of PLA, ABS, PEEK, and PETG's mechanical properties to FDM Printing process parameters. Crystals 11(8):995

38. d6.5d (2000) ASTM D 638. Standard test method for tensile properties of plastics

39. Alberdi A, Suárez A, Artaza T, Escobar-Palafox GA, Ridgway K (2013) Composite cutting with abrasive water jet. Procedia Eng 63:421–429

40. Blundell DJ, Osborn B (1983) The morphology of poly (aryl-ether-ether-ketone). Polymer 24(8):953–958

41. Lambiase F, Scipioni SI, Pace F, Paoletti A (2024) Unraveling the main issues of direct sample printing and sample cutting from a sheet of tensile test samples for characterization of material extrusion components. Int J Adv Manuf Technol 132:2991–3003

42. Scipioni SI, Lambiase F (2023) Error introduced by direct 3D printing of compression samples of PLA made by FDM process. Int J Adv Manuf Technol 129(9–10):4355–4368